CHAPTER 29

WAVE CHARACTERISTICS IN THE SURF ZONE

I.A. Svendsen[1] P.Å. Madsen[2] J. Buhr Hansen[1]

ABSTRACT

The equations describing conservation of mass, momentum and energy in a turbulent free surface flow are derived for a controle volume extending over the whole depth. The effect of the turbulent surface oscillations are discussed but neglected in the following analysis, where the equations are applied to the energy balance in a surf zone wave motion. This leads to results for the wave height variation and the velocity of propagation. The results cannot be reconciled completely with measurements and the concluding discussion is aimed at revealing how the model can be improved.

1. INTRODUCTION

Wave breaking and wave development in the surf zone are topics that have given raise to numerous investigations in the past, and yet much remains to be done before a satisfactory understanding has been obtained and real prediction is possible.

The present paper describes a combined experimental and theoretical work. We concentrate on the development of the gross parameters of wave motion after breaking on a gently sloping beach, and first of all on the phase velocity c and the energy dissipation, i.e. the attenuation of the wave height.

From visual observation aided by photography in laboratory flumes and in the nature it appears that immediately after the wave has started to turn over from the breaking point a violent transition takes place over a horizontal distance of several times the water depth at the breaking point. In this region, which we term the outer breaking region, the motion still shows large scale patterns that are repeated with only small variations from wave to wave (in regular waves) though they of course differ radically with the type of breaking and hence also from wave to wave in an irregular train of waves as on a natural beach. This feature of the breaking process is most significant in a plunging breaker.

From this description it is natural to conjecture that the process is dominated almost entirely by the wave data at the breaking point, i.e. the water depth h_b and wave height H_b. In other words that for a wide range of wave parameters the horizontal scale for the development in this

[1]Assoc. Professor, [2]Ph.D.-student.
Institute of Hydrodynamics and Hydraulic Engineering (ISVA),
Technical University of Denmark, Building 115, DK-2800 Lyngby.

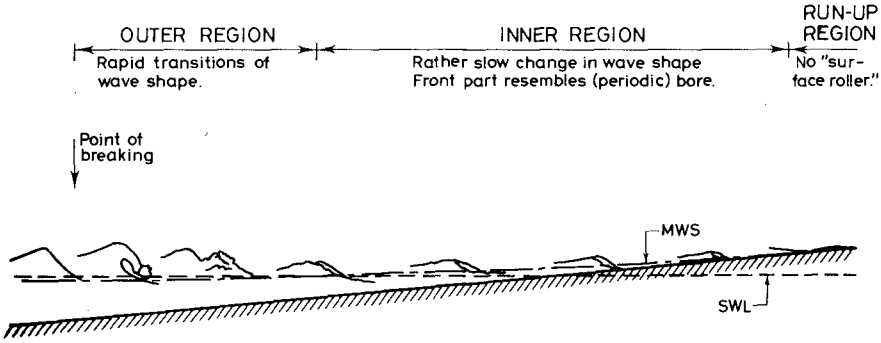

Fig. 1 Wave characteristics in the surf zone.

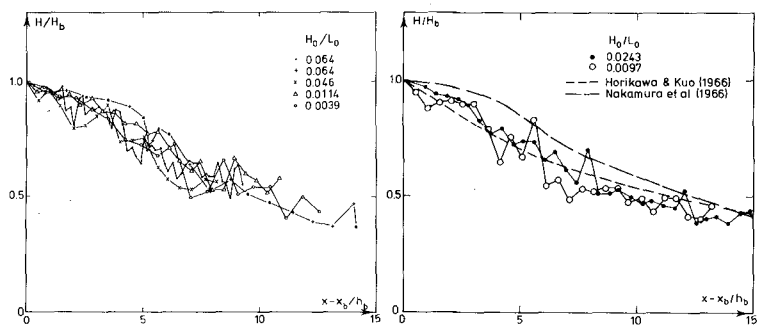

Fig. 2 Relative change in wave height right after breaking.

region is h_b. This is actually confirmed in Fig. 2 which shows the relative change in wave height H/H_b versus the distance from the breaking point measured in units of h_b.

The figure also includes data obtained by Horikawa & Kuo (1966) and by Nakamura et al (1966) on a similar slope (1 in 30 against ours 1 in 34) though the above mentioned conjecture implies that the effect of the slope is insignificant. It is worth noticing that the wide range of wave parameters in Fig. 2 means that the wave height variation is independent of the breaker type (spilling or plunging). Considering the actual differences in the motion one must question the adequacy of the notion "wave height" as a means of description.

As the wave propagates further the large scale deterministic flow breaks up into small scale details which gradually become of a random turbulent nature. During this process the front of the wave becomes

very similar to a moving bore or a hydraulic jump, and we may speak of a system of periodic bores. We term this the inner breaking region and it extends to the shoreline where the run-up starts.

It should perhaps be emphasized that if the wave breaks at or near the shoreline (as e.g. a collapsing or surging breaker) this region is absent and the outer region is immediately followed by the run-up. The description also fails to apply if the depth starts to increase shorewards so the breaking ceases.

One of the remarkable features of the inner region is that the waves or bores from a plunging breaker cannot be distinguished visually from those originating from a spilling breaker.

Thus the water motion at each depth seems to be strongly locally controlled in the sense that local depth and bed slope determines the characteristics of the flow and hence the energy dissipation, the shape of the wave including energy flux, and consequently the decrease in wave height. This hypothesis will find further support in the measurements reported in § 2, where we shall find that for a particular wave train the height to depth ratio H/h is only slowly decreasing and the shape is almost constant in the case of a constant slope.

The internal flow pattern has been studied by Peregrine and Svendsen (1978) who describe the resemblance with in particular hydraulic jumps and single bores occurring in front of a propagating change in water depth. Based on a new flow visualization method they concluded that the turbulence associated with a hydraulic jump or a bore is not limited to a surface roller. In fact there is nothing that separates the surface roller from the rest of a region of highly turbulent flow which originates from the toe of the roller. From there the turbulence develops, in the beginning much like in a turbulent mixing layer. The thickness of the turbulent region increases gradually with distance behind the toe of the roller but remains attached to the free surface. At some distance it reaches the bottom too. These conclusions are supported by the measurements made in a hydraulic jump by Resch et al. (1976).

It is the purpose of this paper to try to explain analytically the basic features phase velocity, energy dissipation rate and wave height attenuation. For this purpose we develop in § 3 the integrated forms of equations describing conservation of mass, momentum and energy and discuss the assumptions made, in particular with respect to the turbulent surface fluctuations.

§ 4 describes how the energy equation can be used to determine the wave height variation and the measurements are used as guidance in the choice of velocity and pressure profiles required in the computations. This also applies to the determination of the velocity of propagation c which turns out to be an important quantity in the description.

The conclusions are not satisfactory yet, and the analysis is succeeded by a discussion of the inaccuracies and possible improvements (§ 8).

2. EXPERIMENTAL RESULTS

The experiments were performed in one of ISVA's 60 cm wide wave flumes (length 32 m) with a water depth at the wave generator of 36 cm's. The waves were of the very regular type deprived of their free second harmonic components (Buhr-Hansen and Svendsen, 1974). The waves broke on a plane slope 1:34 (see Fig. 3) and the surface variations were measured

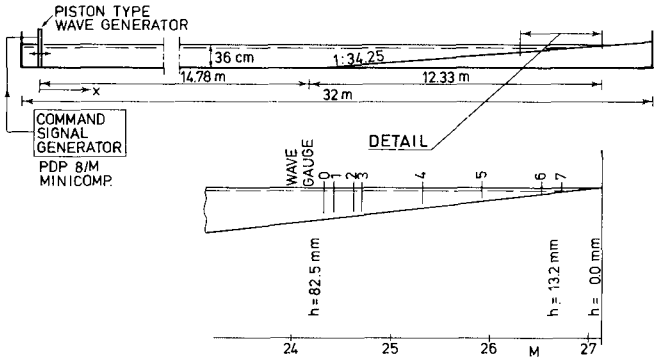

Fig. 3 Experimental set-up.

by resistance gauges (two goldplated silver wires, 0.17 mm diameter, 5 mm apart) and recorded digitally. Eight fixed wave gauges (denoted channel 0, .., 7) were used, positioned as shown in Fig. 3. Only surface elevations were measured and the depth (excluding set-up) range from about 82 mm at channel 0 to about 13 mm at channel 7.

The following account of measurements is only a preliminary presentation. Results of a more detailed and systematical investigation will follow.

First it is worth mentioning that resistance wave gauges can not without further notice be used in water with air entrained as bubbles as we find it around the front of the broken waves. However, detailed investigations have been made in a vessel with controlled air entrainment. The results show that the gauges used to the accuracy required here measure solid water, i.e. measure the elevation we would have had if the air had been absent. Furthermore visual observations of the bubble-water mixture were compared with photos of the front of the waves indicating that the actual air content in the most densely entrained parts of the laboratory wave is only 2-4 per cent.

Thus the surface elevations reported in the following may be regarded as the elevation of water with normal density.

The digital registration makes it possible to identify data points separated an integral number of wave periods, and thus an ensemble average over many waves can be obtained for the profile at each measur-

ing point. Fig. 4 shows such profiles (η) and the standard deviation $\sigma(\eta)$. The results were obtained over 20 wave periods. As expected the

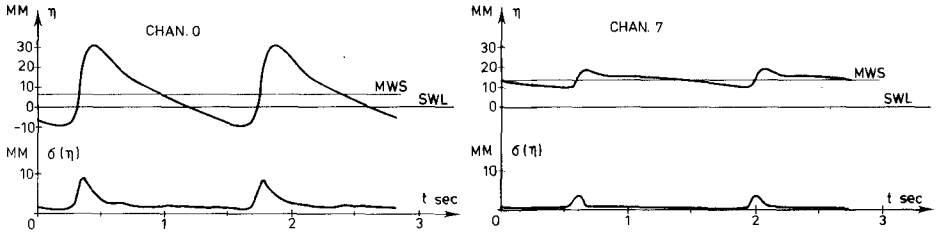

Fig. 4 Mean and standard deviation of measured profiles for experiment with T = 1/.7 sec, H_i = 100 mm.

standard deviation is maximum (about 0.2H, H being wave height) at the front and very small elsewhere. Notice that the variations at the front may well be fluctuations in the horizontal position interpreted as vertical fluctuations by the ensemble averaging procedure.

Fig. 5 shows wave height to mean water depth H/h_{MWS} versus still water depth h_{SWL} in the region considered. The experiments reported have deep water steepnesses H_0/L_0 between 0.0088 and 0.034. Thus the distance from the breaking point varies from test to test. The figure shows that H/h is decreasing slowly and that the value depends on H_0/L_0. Yet the scattering for tests with similar data is considerable, so further investigations are obviously needed for a systematical understanding of this point.

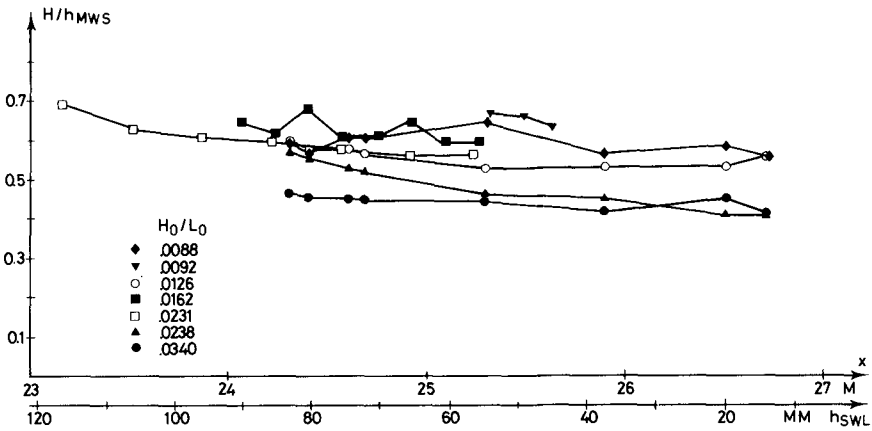

Fig. 5 Variation of wave height to water depth ratio versus still water depth.

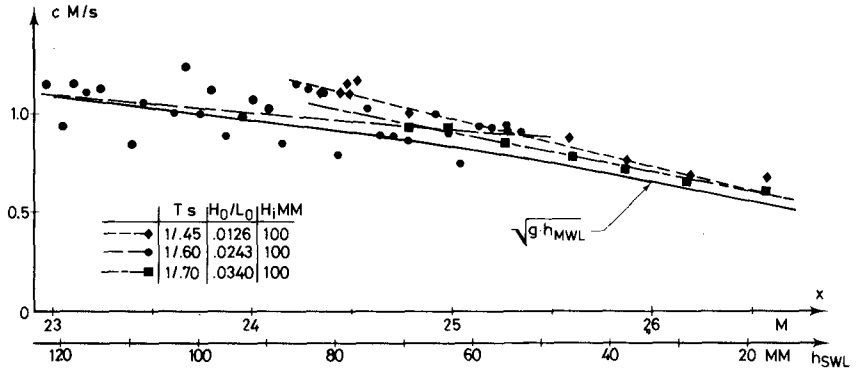

Fig. 6 Measured propagation velocity c.

The measurements of c reported in Fig. 6 were obtained from a trolley moving along the wave flume with two wave gauges 20 cm apart. This set-up measured the propagation time between the two gauges for a point of the wave with a fixed chosen elevation. Results for c versus mean water depth are shown in Fig. 6 with $\sqrt{gh}_{MWS}$ as reference curve. It is tempting though - as we shall see - irrelevant to conclude that the linear shallow water result is a fair approximation (i.e. $c/\sqrt{gh}_{MWS}$ is almost equal to unity).

For each of the 8 recording points (channel 0 through 7) the (ensemble) mean profiles have been determined in each test and Fig. 7 shows such profiles at 4 of the points for 4 different tests, and Fig. 8 shows a comparison of the profiles at the first and the last measuring point. Notice that the abscissa corresponds to increasing time at fixed x so that the wave profiles are "propagating towards the left". The vertical coordinate is scaled with the local wave height to make a direct comparison possible.

The striking feature of these figures is the remarkable similarity of the profiles, not only from point to point in a particular test, but also at the same point for different deep water data (Fig. 8). In fact the only significant development seems to be a decrease in the height of the crest and an increase in depth of the trough as the wave propagates shorewards. Since the surface elevation η is adjusted so that $\int_0^T \eta\, dt = 0$ (i.e. η is measured from the local MWS) these changes do of course correspond to a systematical change in shape. It may be noticed that this development goes in the direction of a linear variation of η between crest and trough.

In the following sections we try to understand the physical flow conditions behind these results on the basis of the fundamental equations of hydrodynamics.

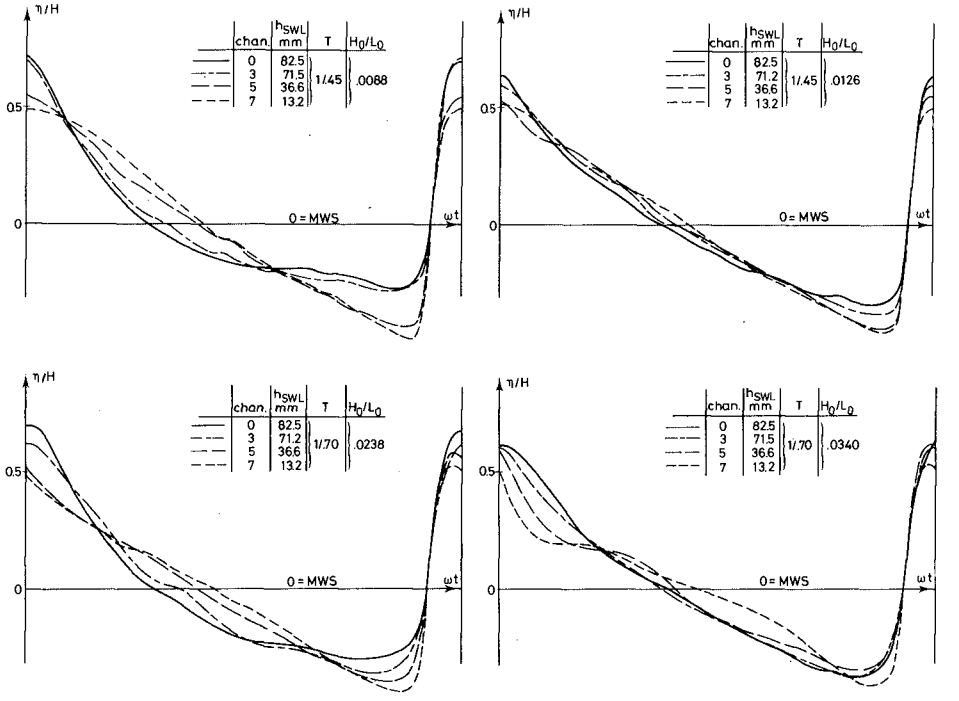

Fig. 7 Mean profiles at four different points.

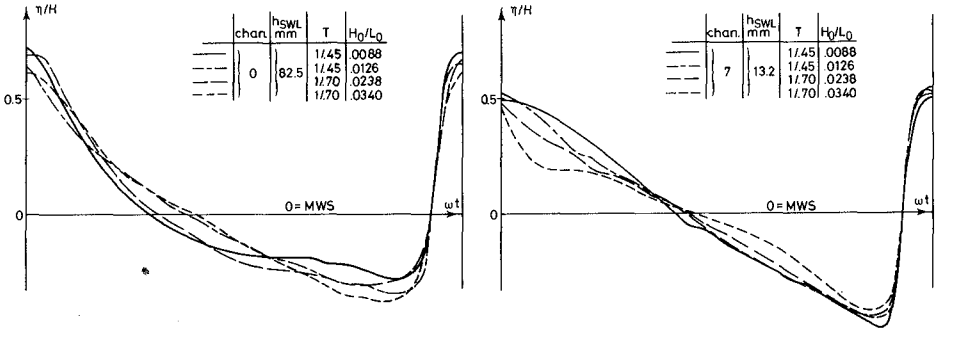

Fig. 8 Mean profiles for different experiments at channel 0 and channel 7.

3. THE INTEGRATED EQUATIONS

As described in the introduction the motion of the waves in the inner region of the surf zone resembles periodic bores or hydraulic jumps. Thus it is natural to start a theoretical analysis by applying the same methods as have been used with great success on particularly hydraulic jumps, i.e. using the integrated equations of mass and momentum to determine the velocity of propagation c and the integrated energy equation to find the dissipation.

Before doing so it is profitable to consider the form of these basic equations. In this context we briefly mention some effects at the free surface which are due to the turbulence, and which do not seem yet to be widely appreciated.

The coordinates and notation used in the following are shown in Fig. 9, which also indicates the type of problem considered.

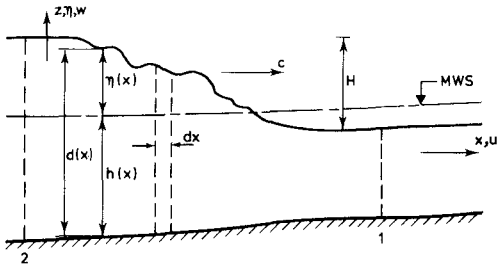

Fig. 9 Definition sketch.

The integrated equations for conservation of mass, momentum and energy may be derived from the general formulation of these principles given by Jeffrey (1965) for volumes with boundaries moving arbitrarily relative to a fixed frame of reference.

For reference these equations are quoted in our notation and for our conditions, i.e. an incompressible fluid without interval energy (neuclear, chemical, etc.).

Equation of continuity

$$\frac{\partial}{\partial t}\int_{V(t)} \rho \, d\omega + \int_{S(t)} (\vec{u} - \vec{v}) \cdot d\vec{S} = 0 \qquad (1)$$

Equation of momentum

$$\frac{\partial}{\partial t}\int_{\Omega(t)} \rho \vec{u} \, d\omega = - \int_{S(t)} p \, d\vec{S} - \int_{S(t)} \rho \vec{u} (\vec{u}-\vec{v}) \cdot d\vec{S} + \int_{\Omega(t)} \rho \vec{g} \, d\omega \qquad (2)$$

Equation of energy

$$\frac{\partial}{\partial t}\int_{\Omega(t)} \rho \vec{u}^2/2 \, d\omega = - \int_{S(t)} p\vec{u} \cdot d\vec{S} - \int_{S(t)} \rho u^2/2 (\vec{u}-\vec{v}) \cdot d\vec{S}$$

$$+ \int_{\Omega(t)} \rho \vec{u} \cdot \vec{g} \, d\omega - \int_{\Omega(t)} D_V \, d\omega \qquad (3)$$

Here $S(t)$ is the surface of the controle volume $\Omega(t)$, $\vec{u}$ is the fluid velocity and $\vec{v}$ the velocity of the surface element $d\vec{S}$ (for a volume changing in time) positive along the outward normal. D_V is the energy dissipation per unit volume due to viscous forces. In the equation of momentum viscous stresses along the surface have been neglected in this formulation.

For waves on a sloping bottom it appears to be simplest to use a control volume (see Fig. 9) following the free surface but otherwise being fixed in space, at first of length dx, later on integrated over a finite horizontal distance. (Thus the first step corresponds to an integration over depth of the differential form of the three equations).

The continuity equation

From (1) the continuity equation becomes

$$\frac{\partial}{\partial t}\int_{-h}^{\eta} \rho\, d z + \frac{\partial}{\partial x}\int_{-h}^{\eta} \rho u\, d z = 0 \tag{4}$$

which results in the well known

$$\frac{\partial}{\partial x}\int_{-h}^{\eta} u\, d z = -\eta_t \tag{5}$$

In this equation we now extract the turbulent fluctuation denoted by '. Thus we in general introduce

$$(u,w,p,\eta) = (\bar{u},\bar{w},\bar{p},\bar{\eta}) + (u',w',p',\eta') \tag{6}$$

where $\bar{}$ means time mean value.

In (5) this yields after turbulent time averaging (i.e. disregarding the time variation of the mean values)

$$\frac{\partial}{\partial x}\int_{-h}^{\bar{\eta}} u\, d z = -\frac{\partial \eta}{\partial t} - \frac{\partial}{\partial x}\overline{\int_{\bar{\eta}}^{\bar{\eta}+\eta'} u\, d z} \tag{7}$$

The last term here actually corresponds to the extra term found by Hasselmann (1971) in the kinematic free boundary condition in a situation with wavelets superimposed on larger scale wave motions.

Notice that the result (7) is readily obtained by an integration over depth of the continuity equation $\nabla \cdot \bar{u} = 0$ if Hasselmann's kinematic boundary is used at the turbulent mean surface $\bar{\eta}$.

Obviously similar terms must occur in the equations of momentum and energy. Hasselmann also showed that the dynamic free surface condition at $z = \bar{\eta}$ is not $\bar{p}(\bar{\eta}) = 0$, but

$$p(\eta) = -\rho\overline{w'^2} \tag{8}$$

a change which is again a result of the fluctuations at the turbulent mean water surface $\bar{\eta}$.

In all published investigations on bores and hydraulic jumps known to the authors (as e.g. Resch, Leutheusser and Coantin, 1976, Rouse, 1958, Tsubaki, 1950) the fluctuations in η seem to have been neglected, corresponding to omission of the last term in (7) and similar terms in the other equations. In an ordinary free surface turbulent flow these

terms are probably small, but this can hardly be expected to apply to the region with the surface roller in a hydraulic jump or a bore.

Thus being aware of the possible errors it may lead to, we shall in the present investigation allow ourselves to make the same approximation (i.e. neglect the effect of the surface fluctuations) in order to be able to pursue other ideas. We therefore assume that the continuity equation reads

$$\frac{\partial}{\partial x}\int_{-h}^{\bar{\eta}} \bar{u}\, dz = -\bar{\eta}_t \tag{9}$$

in which we may substitute the definition

$$U \equiv \frac{1}{d}\int_{-h}^{\bar{\eta}} \bar{u}\, dz \tag{10}$$

to get

$$\boxed{\frac{\partial}{\partial x}(U\, d) = -\bar{\eta}_t} \tag{11}$$

The equation of momentum

From (2) we get

$$\frac{\partial}{\partial t}\int_{-h}^{\eta} \rho\, dz = -\frac{\partial}{\partial x}\int_{-h}^{\eta}(\rho u^2 + p)dz + h_x\, p(-h) - \tau_b \tag{12}$$

which is exact since $p(\eta)$ is zero. τ_b is the bottom shear stress. Introducing the turbulent description by substituting (6), and neglecting the fluctuations of the free surface yields after turbulent averaging

$$\frac{\partial}{\partial t}\int_{-h}^{\bar{\eta}} \bar{u}\, dz + \frac{\partial}{\partial x}\int_{-h}^{\bar{\eta}} (\bar{u}^2 + \overline{u'^2} + \bar{p})dz - \frac{1}{\rho}h_x\, p(-h) + \tau_b = 0 \tag{13}$$

For further applications it is convenient to express the integrals in terms of coefficients, which we define as

$$\alpha = \frac{1}{d}\int_d (\bar{u}/U)^2 dz \;; \qquad \alpha' = \frac{1}{d}\int_d \overline{u'^2}/U^2\, dz \tag{14}$$

$$\kappa^+ = \frac{1}{\rho g d^2}\int_d p^+ dz \qquad \text{where} \qquad p^+ = \bar{p} + \rho g z \tag{15}$$

Thus (13) may be written

$$\boxed{\rho\frac{\partial}{\partial t}(Ud) + \frac{\partial}{\partial x}[\rho(\alpha+\alpha')d\, U^2 + \rho g \kappa^+ d^2 - \frac{1}{2}\rho g \bar{\eta}^2] - h_x\, p^+(-h) + \tau_b = 0} \tag{16}$$

Here the $\partial/\partial t$ - term can not be integrated with respect to x without information or assumptions about the changing shape of the wave. This is discussed in the following paragraphs.

The energy equation

Here it is useful first to consider the $\vec{g}$ - term in (3). This term

in fact represents the potential energy and may conveniently be rewritten as follows

$$\int_{\Omega(t)} \rho \vec{u} \cdot \vec{g} \, d\omega = - \int_{\Omega(t)} \rho \vec{u} \cdot \nabla g z \, d\omega$$

which invoking the continuity equation $\nabla \cdot \bar{u} = 0$ becomes

$$= - \int_{\Omega(t)} (\nabla \cdot g z \vec{u}) d\omega = - \int_{S(t)} E_p \vec{u} \cdot d\vec{S} \tag{17}$$

with $E_p \equiv g z$ (18)

We further notice that the rate of change of potential energy inside the volume is

$$\frac{\partial}{\partial t} \int_{\Omega(t)} E_p \, d\omega = - \int_{\Omega(t)} \rho \vec{u} \cdot \vec{g} \, d\omega + \int_{S(t)} E_{pot} (\vec{v} - \vec{u}) \cdot d\vec{S} \tag{19}$$

where the minus sign of the first right hand term indicates that gravity has to do negative work to increase the potential energy. Combining (17) and (19) yields

$$\int_{\Omega(t)} \rho \vec{u} \cdot \vec{g} \, d\omega = - \frac{\partial}{\partial t} \int_{\Omega(t)} E_p \, d\omega + \int_{S(t)} E_p (\vec{v} - \vec{u}) \cdot d\vec{S} \tag{20}$$

When substituted into (3) this can be written

$$\frac{\partial}{\partial t} \int_{\Omega(t)} (E_k' + E_p) d\omega = - \int_{S(t)} p \vec{u} \cdot d\vec{S} - \int_{S(t)} (E_k' + E_p) (\vec{u} - \vec{v}) \cdot d\vec{S} - \int_{\Omega(t)} D_V \, d\omega \tag{21}$$

with

$$E_k' \equiv \frac{1}{2} \rho \vec{u}^2 \tag{22}$$

For the particular control volume considered here we get in the first step (length dx, see Fig. 9)

$$\rho \frac{\partial}{\partial t} \int_{-h}^{\eta} (E_k' + E_p) dz = - \frac{\partial}{\partial x} \int_{-h}^{\eta} (p + E_k' + E_p) u \, dz - \int_{-h}^{\eta} D \, dz \tag{23}$$

When we in (23) substitute the turbulent description (6) and average, a large number of turbulent fluctuation terms result. These, however, all belong to the category which we in this context include in the dissipation term D. Thus we concentrate our attention on the ordered mechanical energy only and therefore get

$$\frac{\partial}{\partial t} \int_{-h}^{\bar{\eta}} (E_k + E_p) dz = - \frac{\partial}{\partial x} \int_{-h}^{\bar{\eta}} (p + E_p + E_k) u \, dz - \int_{-h}^{\bar{\eta}} D_t \, dz \tag{24}$$

with

$$E_k \equiv \frac{1}{2} \rho (\bar{u}^2 + \bar{w}^2) \tag{25}$$

in which D_t now includes both viscous dissipation and turbulent energy

not yet dissipated, and we recognize the well known expression for the flux of ordered mechanical energy

$$E_f(t) = \int_{-h}^{\bar{\eta}} (\rho g z + \bar{p} + \tfrac{1}{2}\rho(\bar{u}^2 + \bar{w}^2))\bar{u}\, dz \tag{26}$$

Thus the energy equation may be written

$$\frac{\partial}{\partial t}\mathcal{E} = -\frac{\partial}{\partial x} E_f(t) - \mathcal{D} \tag{27}$$

with the definitions

$$\mathcal{E} = \int_{-h}^{\bar{\eta}} (E_k + E_p)dz \; ; \; \mathcal{D} = \int_{-h}^{\bar{\eta}} D_t\, dz \tag{28}$$

which simply states that the rate of change of energy inside the control volume is the difference between net flux over the boundary and the loss due to dissipation.

Again it is useful to express the integrals in terms of coefficients which we define as

$$\beta = \frac{1}{d}\int_d (\bar{u}^3 + \bar{w}^2\, \bar{u})/U \quad dz \tag{29}$$

$$\delta = \frac{1}{\rho g d^2}\int_d (\bar{u} - U)p^+/U\, dz \tag{30}$$

Then the energy flux $E_f(t)$ may be written

$$E_f(t) = \int_{-h}^{\bar{\eta}} (p^+ + \tfrac{1}{2}\rho\,(\bar{u}^2 + \bar{w}^2)\bar{u}\, dz = \rho g d^2 U(\delta + \kappa^+) + \rho\beta d U^3 \tag{31}$$

and the energy equation becomes

$$\boxed{\frac{\partial}{\partial t}\mathcal{E} = -\frac{\partial}{\partial x}[\rho g d^2 U(\delta + \kappa^+) + \rho\beta d U^3] - \mathcal{D}} \tag{32}$$

Thus it has been shown how the three fundamental equations integrated over depth can be expressed in terms of velocity and pressure profiles under the assumptions mentioned. In the following these equations are applied to waves.

4. AVERAGED ENERGY EQUATION

One of the important features in the surf zone is the wave height attenuation due to the turbulence generated by the breaking.

For this purpose we average (27) over a mean period (assuming periodicity in time) to get

$$\bar{\mathcal{D}} = -\frac{\partial E_f}{\partial x} \tag{33}$$

where $\bar{\mathcal{D}}$ is the mean dissipation per m^2 of bottom and E_f is the time mean of $E_f(t)$. We define a non dimensional energy flux B in analogy to ordinary wave theory and using (26) find

$$E_f = \frac{1}{T}\int_0^T \int_{-h}^{\bar{\eta}} (p^+ + \frac{1}{2}\rho(\bar{u}^2 + \bar{w}^2))\bar{u}\,dz\,dt \equiv \rho g c H^2 B \tag{34}$$

Similarly we define a nondimensional energy dissipation D and since we want to relate this quantity to the hydraulic jump or bore conditions it is convenient to let D represent the energy dissipation per wave length. Thus we write

$$\bar{\mathcal{D}} \equiv \rho g \frac{c}{L}\frac{H^3}{4h} D \tag{35}$$

a form which is closely related to the expression for the hydraulic jump.

Substitution of (34) and (35) into (33) and rearrangement of the terms yield

$$\left(\frac{H}{h}\right)_X = -\left(\frac{h_x}{h} + \frac{c_x}{2c} + \frac{B_x}{2B}\right)\frac{H}{h} - \frac{h_0}{8L}\frac{D}{B}\left(\frac{H}{h}\right)^2 \quad ; \quad X = \frac{x}{h_0} \tag{36}$$

which is a first order nonlinear differential equation in H/h. Notice that (36) itself is fairly general. It is only assumed that the motion is periodic and that D includes the turbulent energy. It also turns out to be a quite convenient basis for studying the effect of simplifying assumptions, also in the related expressions (31) and (34) for B. Solution, however, requires information of the coefficients, and this is the purpose of the following analysis.

The h_x/h term includes the wave set-up so that determination of this term requires integration of the averaged form of the equation of momentum (16). This is perfectly possible but is considered beyond the scope of the present paper. Since the set-up in most of the surf zone is only a small fraction of the still water depth we use an estimate of h_x/h based on the bottom slope and experimental results for the set-up.

The $c_x/2c$ and $B_x/2B$ are more interesting terms, and we first tackle the determination of c.

5. THE VELOCITY OF PROPAGATION

For simplicity the method by which c can be determined for a breaking wave is described for constant depth only. It should be mentioned, however, that it is fairly straightforward to show that the effect of a sloping bottom is negligible on c.

We also assume that the wave motion is of constant form to avoid the complications of defining a speed of propagation for a changing wave form and include the associated effects in the analysis. With a proper choice of c (speed for $\eta = 0$, say) the effect would again be negligible.

None of these assumptions in fact remove from the problem the effects we want to study, namely the influence of the velocity and pressure variation over the depth (i.e. the magnitude of α and κ and for the energy dissipation of β and δ).

Under these conditions it is convenient to change to a frame of reference moving with the wave, and in which the horizontal particle velocity is termed v. Thus

$$\left.\begin{aligned} &v = u - c \quad ; \quad V = U - c \\ &\alpha^V = \frac{1}{d}\int_d (v/V)^2\, dz \end{aligned}\right\} \quad (37)$$

In a wave of constant form we have

$$\int_d u\, dz = U d = c\bar{\eta} \quad (38)$$

if i) $\bar{\eta}$ is measured from the mean water level

ii) there is no net mass flux

(see Svendsen, 1974, p. 164 ff).

The continuity equation (11) yields

$$V d = \text{const} = (U - c)d = c\bar{\eta} - c d$$

or

$$V = - c h/d \quad (39)$$

h being the mean water depth.

The equation of momentum (16) becomes (neglecting the bottom friction)

$$\frac{\partial}{\partial t}(V d) + \frac{\partial}{\partial x}[(\alpha^V + \alpha')d V^2 + g\kappa^+ d^2 - \frac{1}{2}g\bar{\eta}^2] = 0 \quad (40)$$

in which the constant form assumption implies that $\partial/\partial t = 0$ so that the equation can be integrated from x_2 to x_1 (see Fig. 9) to yield

$$(\alpha^V + \alpha')d V^2 + g\kappa^+ d^2 - \frac{1}{2}g\bar{\eta}^2\Big]_2^1 = 0 \quad (41)$$

or with V from (39)

$$c^2h^2/d\ (\alpha^V + \alpha') + g\kappa^+ d^2 - \frac{1}{2}g\bar{\eta}^2\Big]_2^1 = 0 \quad (42)$$

For a wave of constant form c is the same for any choice of x_1 and x_2. Hence (42) is an equation from which c may be determined, the proper information given. (A check on a solitary wave, say, rapidly confirms this).

In numerical computations, however, the most accurate results are obtained when x_2 and x_1 are placed at the (instantaneous) position of the crest and trough, respectively (Fig. 9).

As a special case we first consider a periodic bore with static pressure and v uniform over the depth. Placing x_2 so far down the stream that there is no turbulence we have

$$\alpha^V = 1 \quad ; \quad \alpha' = 0 \quad ; \quad \kappa^+ = \eta/d \quad (43)$$

Solving for c we then get

$$\frac{c^2_{bore}}{gh} = \frac{1}{2}\frac{d_1 d_2}{h^3}(d_1 + d_2) \quad (44)$$

or with $\zeta = d_2/d_1$; $\zeta_t = d_1/h$ (45)

$$\frac{c^2_{bore}}{gh} = \frac{1}{2}\,\zeta_t^3\,\zeta(\zeta + 1) \tag{46}$$

which transforms into the well known expression for a single bore if we choose $h = d_1$ (i.e. $\zeta_t = 1$).

In the more general case the direct solution of (42) yields

$$\frac{c^2}{c^2_{bore}} = A_1\left[1 + 2\,\frac{\kappa_2\zeta - \kappa_1}{\zeta^2 - 1}\right]$$

where by definition (47)

$$\kappa \equiv \kappa^+ - \bar{\eta}/d \quad ; \quad A_1 \equiv \frac{\zeta - 1}{(\alpha_1^v + \alpha_1') - (\alpha_2^v + \alpha_2')}$$

index $_{1,2}$ referring to x_1 and x_2 respectively and c_{bore} given by (46).

In (47) may now be introduced various assumptions for the α^v and κ coefficients and the outcome compared with the measurements reported in § 2. Fig. 10 shows the result of such computations. Here three different sets of coefficients have been used, and for reference $\sqrt{g\,h}$ is shown too.

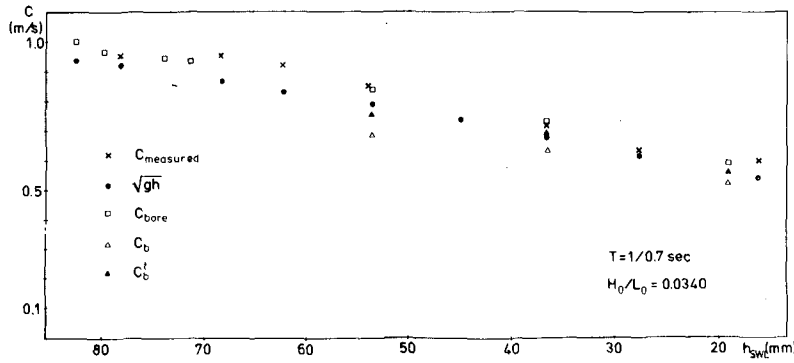

Fig. 10 Measured and computed values of c.

The results denoted c_{bore} correspond to (46). The values of $\bar{\eta}$ used in the computation were taken from the measured profiles and we see that the agreement is good, but of course this can not be taken as a proof of static pressure and uniform velocity.

The points denoted c_B have been obtained by assuming a deviation from static pressure corresponding to a Boussinesq approximation. Thus for $\bar{u}$ we have used

$$\bar{u} = c\,\bar{\eta}/d + \frac{1}{2}\left(\frac{1}{3} - \left(\frac{z+h}{d}\right)^2\right) h\,\bar{\eta}_{xx} \tag{48}$$

and for $\bar{p}$

$$\bar{p} = \rho g[(\bar{\eta} - z) + \frac{1}{2}(1 - (\frac{z+h}{d})^2 h \bar{\eta}_{xx}] \tag{49}$$

Again the values of $\bar{\eta}$ and $\bar{\eta}_{xx}$ have been determined from the measured mean profiles.

As Fig. 10 shows the resulting c-values are smaller than the bore velocity. In general a non uniform velocity profile under the wave crest (x_2) (as (48)) yields $\alpha^v > 1$, which tends to increase c, whereas a pressure lower than static ($\kappa < 0$) will reduce c. (In the trough (x_1) the value of $h\eta_{xx}$ is too small to give significant contributions).

In c_{bore} and c_B the turbulence has been neglected by assuming $\alpha' = 0$.

The last set of points (denoted c_B^t shows the effect of the turbulent velocity fluctuations. The value of α' has been chosen as 0.10, which is the approximate value one can derive from Rasch et al. (1976) who report results for $\overline{u'^2}$ in a hydraulic jump.

The turbulent velocity fluctuations act as an additional momentum and hence increase c. In the figure α' has been applied to the case where α^v and κ were determined by a Boussinesq approximation (so c_B^t should be compared with c_B). In the classical sense this is inconsistent since the Boussinesq theory is usually based on potential theory. However, the formula (49) may also be derived simply by assuming a linear variation of the curvature of the mean stream lines, and (48) may be regarded as simply a parabolic approximation for $\bar{u}$.

In general the effect of turbulence (i.e. α') on c can be extracted from (47) as

$$\frac{c^{turb}}{c_{potential}} = (1 - \frac{\alpha'}{\zeta - \alpha})^{-1/2} \tag{50}$$

It is emphasized here that $\alpha' = 0.10$ is not much more than an arbitrary guess used to illustrate the nature of the problem.

6. THE ENERGY FLUX

The non dimensional energy flux B can be determined from (34) using the same type of information required to find c. When (31) is substituted B is expressed in terms of the coefficients β, δ and κ^+ and by U, $c^2/g\,h$ and H, and the result can be tidied for waves of constant form using the continuity equation.

Here it suffices to mention that for sections (x_2, x_1) at crest and trough $\bar{w} \sim 0$, and if we introduce the linear shallow water assumptions

$$u \sim c\,\bar{\eta}/h \quad ; \quad p^+ \sim \rho g \bar{\eta} \tag{51}$$

we get as first approximation for B

$$B = \frac{1}{T} \int_0^T (\bar{\eta}/H)^2 \, dt \tag{52}$$

Let us for a moment consider improvements of this result using the

Boussinesq approximation introduced above. Then (52) is the first term in an expansion in η/H. Further analysis shows that the next term with $(\eta/H)^3$ yields contributions only a few percent of (52), for measured values of η.

Therefore in the following considerations it seems reasonable at the present stage to rely upon (52) for B.

7. WAVE HEIGHT VARIATION AND ENERGY DISSIPATION

The application of (36) to determine the wave height variation requires input for the energy dissipation described by D, and considering that c was found to be nearly equal to c_{bore} the first natural choice is also to use the bore result for the energy dissipation. For a periodic bore this corresponds to

$$D = h^2/d_1 d_2 \tag{53}$$

Fig. 11 shows the resulting variation in the wave height compared with

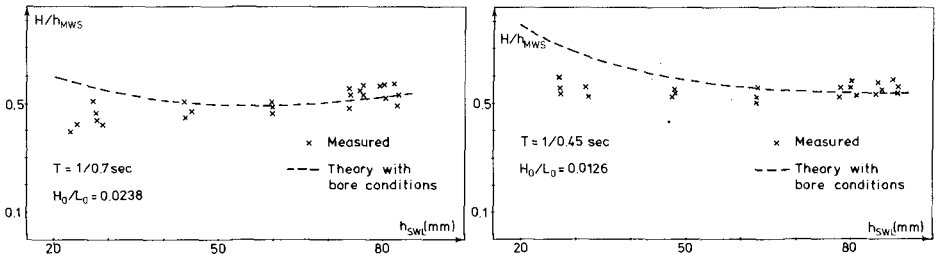

Fig. 11 Measured and computed ratios of wave height to water depth H/h.

measured results. As input to the computations is used the wave height at the first measuring point (largest depth). The agreement is poor and obviously the energy dissipation can not be determined by simple bore relations.

To further illustrate this (36) has been reversed by solving with respect to the D-term which is then determined by using measured values of the other terms including $(H/h)_X$. We define

$$\Delta E_{measured} \equiv \frac{h_0}{8L}\left(\frac{H}{h}\right)^2 \frac{D}{B}$$
$$= -\left(\frac{H}{h}\right)_X - \frac{H}{h}\left(\frac{h_X}{h} + \frac{c_X}{2c} + \frac{B_X}{2B}\right) \tag{54}$$

Fig. 12 shows a comparison between $\Delta E_{measured}$ and ΔE_{bore} which clearly confirms the conclusion above.

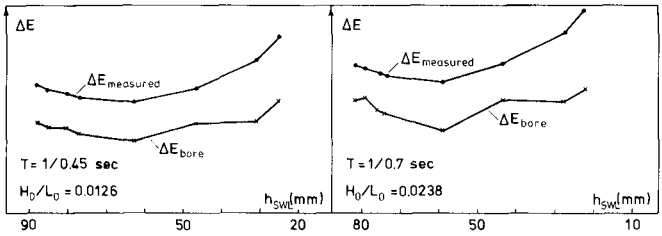

Fig. 12 Measured and computed values of ΔE defined by Eq. 54.

The actual energy dissipation may be determined from (32) for simplifying assumptions similar to those introduced to find (47) for c. And again these represent a good approximation locally. Thus neglecting the changing form of the wave and assuming a horizontal bottom $\partial\mathcal{E}/\partial t$ becomes equal to $-c\,\partial\mathcal{E}/\partial x$ and (32) integrates directly from x_2 to x_1. The result represents an equation with the term $\int_{x_2}^{x_1} \mathcal{D}\,dx$ as unknown. This term represents the total energy dissipation between x_2 and x_1. The solution can be written in terms of D introduced above as

$$\frac{D}{D_{bore}} = 1 + \frac{2}{(\zeta-1)^2}(\zeta^2\kappa_2 + \kappa_1) + A_3\left(\frac{\zeta+1}{\zeta-1}\right)^2\left[1 + \frac{2}{\zeta^2-1}(\zeta^2\kappa_2 - \kappa_1)\right]$$

$$- 4\,\frac{\zeta}{(\zeta-1)^3}(\zeta\,\delta_2^V - \delta_1^V) \qquad (55)$$

where

$$A_3 = A_1\frac{\zeta^2\,\beta_1^V - \beta_2^V}{\zeta^2 - 1} - 1$$

with β^V and δ^V defined from (29) and (30) in analogy with (37), and κ and A_1 by (15) and (47) respectively.

In (55) a uniform velocity distribution corresponds to $\delta = 0$, $A_3 = 0$ and $A_1 = 1$, and static pressure implies $\kappa = 0$, $\delta = 0$.

8. DISCUSSION

Eqs. 47 and 55 have been evaluated for a variety of velocity and pressure conditions in order to obtain agreement with the measurements. This would require a D/D_{bore} value of 1.4 to 1.6 corresponding to the ratio between the two curves in Fig. 12, and at the same time c must be close to c_{bore} as indicated by Fig. 10.

In this context the physical picture of the process suggested by Peregrine and Svendsen (1978) (see description in § 1) has been invoked.

This model implies that at the bottom between x_2 and x_1 the flow is not influenced by the (surface) turbulence, so that the Bernoulli equation yields a simple relation between the bed velocities at x_2 and x_1, (pressure specified). In all cases considered the conditions at the wave trough were fixed at static pressure and uniform horizontal velocity.

The following general properties may be extracted from these investigations:

a) D/D_{bore} increases for increasing values of α_2^v. On the other hand any physically relevant velocity profile yields α^v not much larger than unity. The opposite applies to the pressure variation where pressures smaller than the static at x_2 reduce D/D_{bore}.

b) In this respect D/D_{bore} follows c/c_{bore}. It also appears that the largest value of D/D_{bore} for a fixed value c/c_{bore} is obtained if $|\beta^v|$ is minimized for fixed α^v.

c) None of the relevant velocity profiles and the associated pressure variations, however, lead to D/D_{bore} larger than about 1.2 as long as $\alpha' = 0$ (i.e. as long as the momentum of the turbulent velocity fluctuations are omitted).

d) Notice that the energy dissipation (55) includes the turbulent energy generated between x_1 and x_2 and subsequently convected out of the volume through section 2 (see Fig. 9). But (55) does <u>not</u> include the energy lost by generation of turbulent energy <u>behind</u> section 2. This amount is difficult to estimate but may account for some of the deficit in energy dissipation.

e) Finally it turns out that D/D_{bore} given by (55) increases rapidly with increasing α', i.e. if the momentum of the turbulent fluctuations are included, even though we have seen that the velocity of propagation c is relatively insensitive to this factor.

Though a more detailed investigation of this is required it seems obvious that the significant deviations between measured and calculated energy dissipations shown in Fig. 12 are primarily associated with the momentum of the turbulent velocity fluctuations represented by α'. Further analysis, however, will also require that the effect of the free surface fluctuations are included.

9. REFERENCES

Buhr Hansen, J and Svendsen, I.A. (1974). Laboratory generation of waves of constant form. Proc. 14'th Coast. Engng. Conf., Copenhagen, vol. I, p. 321-339.

Hasselmann, K (1971). On the mass and momentum transfer between short gravity waves and larger-scale motions. Jour. Fluid Mech., 50, p. 189-205.

Horikawa, K. and Kuo, C. (1966). Wave transformation after a breaking point. Proc. 10th Coast. Engng. Conf., Tokyo, chap. 15, p. 217-233.

Jeffrey, A. (1965). A note on the integral form of the fluid dynamic conservation equations relative to an arbitrarily moving volume. ZAMP, vol. 16, p. 835-37.

Nakamura, M. et al. (1966). Wave decaying due to breaking. Proc. 10th Coast. Engng. Conf., Tokyo, chap. 16, p. 234-253.

Peregrine, D.H. and Svendsen, I.A. (1978). Spilling breakes, bores and hydraulic jumps. Proc. 16th Coast. Engng. Conf., Hamburg.

Resch, F.J., Leutheusser, H.J. and Coantic, M. (1976). Etude de la structure cinematique et dynamique du ressaut hydraulique. Journal of Hydraulic Research, 14, 4, p. 293-319.

Rouse, H., Siao, T.T. and Nagaratnam, S. (1958). Turbulence characteristics of the hydraulic jump. Transaction for the Asce, vol. 124, p. 926-950.

Svendsen, I.A. (1974). Cnoidal waves over a gently sloping bottom. Series paper no. 6, Inst. Hydrodyn. and Hydraulic Engrg., Tech. Univ. Denmark.

Tsubaki, T. (1950). Theory of hydraulic jump. Reports, Research Institute for Fluid Engineering, Kyushu University, Fukuoka, Japan, vol. VI, no. 2.